Author Manuscript

Author Manuscript

Author Manuscript

Author Manuscript

HHS Public Access

Author manuscript

Ann Surg Oncol. Author manuscript; available in PMC 2018 September 01.

Published in final edited form as:

Ann Surg Oncol. 2017 September ; 24(9): 2482–2490. doi:10.1245/s10434-017-5896-1.

Computed Tomography Image Texture: A Noninvasive Prognostic Marker of Hepatic Recurrence After Hepatectomy for Metastatic Colorectal Cancer

Amber L. Simpson, PhD[1], **Alexandre Doussot, MD**[1], **John M. Creasy, MD**[1], **Lauryn B. Adams, BS**[1], **Peter J. Allen, MD**[1], **Ronald P. DeMatteo, MD**[1], **Mithat Gönen, PhD**[3], **Nancy E. Kemeny, MD**[4], **T. Peter Kingham, MD**[1], **Jinru Shia, MD**[5], **William R. Jarnagin, MD**[1], **Richard K. G. Do, MD, PhD**[2], and **Michael I. D'Angelica, MD**[1]

[1]Department of Surgery, Memorial Sloan Kettering Cancer Center, New York, NY

[2]Department of Radiology, Memorial Sloan Kettering Cancer Center, New York, NY

[3]Department of Epidemiology & Biostatistics, Memorial Sloan Kettering Cancer Center, New York, NY

[4]Department of Medicine, Memorial Sloan Kettering Cancer Center, New York, NY

[5]Department of Pathology, Memorial Sloan Kettering Cancer Center, New York, NY

Abstract

Background—Recurrence after resection of colorectal liver metastases (CRLMs) occurs in up to 75% of patients. Preoperative prediction of hepatic recurrence may inform therapeutic strategies at the time of initial resection. Texture analysis (TA) is an established technique that quantifies pixel intensity variations (heterogeneity) on cross-sectional imaging. We hypothesized that tumoral and parenchymal changes that are predictive of overall survival (OS) and recurrence in the future liver remnant (FLR) can be detected using TA on preoperative computed tomography images.

Methods—Patients who underwent resection for CRLM between 2003 and 2007 with appropriate preoperative computed tomography scans were included (n=198) in this retrospective study. Texture features extracted from the tumor and FLR and clinicopathologic variables were incorporated into a multivariable survival model.

Results—Quantitative imaging features of the FLR were an independent predictor of both OS and hepatic disease-free survival. Tumor texture showed significant association with OS. TA of the FLR allowed patient stratification into two groups with significantly different risks of hepatic recurrence (HR, 2.09; 95% CI, 1.33–3.28; p=0.001). Patients with homogeneous parenchyma had approximately twice the risk of hepatic recurrence (41% vs. 20%).

Conclusion—TA of the tumor and FLR are independently associated with OS. TA of the FLR is independently associated with HDFS. Patients with homogeneous parenchyma had a significantly

Corresponding author: Amber L. Simpson, PhD, Assistant Attending Computational Biologist, Hepatopancreatobiliary Surgery, Memorial Sloan Kettering Cancer Center, simpsonl@mskcc.org Tel: 212-639-6133 Fax: 212-639-4031.

Author Manuscript Author Manuscript Author Manuscript Author Manuscript

higher risk of hepatic recurrence. Preoperative TA of the liver represents a potential biomarker to identify patients at risk of liver recurrence after resection for CRLM.

Keywords

image analysis; radiomics; liver surgery; quantitative imaging

Introduction

Approximately 140,000 cases of colorectal cancer are diagnosed annually in the United States.[1] Nearly 25% of patients have colorectal liver metastases (CRLMs) at presentation, and approximately 50% to 60% will develop metachronous CRLM.[2] For selected patients with CRLM, hepatic resection is the treatment of choice because of potential long-term survival and cure.[3] Overall recurrence rates, however, are as high as 75%, and at least half of recurrences involve the remnant liver.[4–6] Therefore, predicting, identifying, and treating hepatic recurrence are of critical importance.

Adjuvant hepatic arterial infusion (HAI) chemotherapy with floxuridine (FUDR) and systemic 5-fluorouracil (5-FU) has been associated with improved overall survival (OS), compared to with adjuvant 5-FU alone, in a randomized trial.[7] Furthermore, adjuvant HAI-FUDR is associated with an improvement in hepatic disease–free survival (HDFS) after hepatic resection.[7,8] Thus, preoperative prediction of hepatic recurrence would identify candidates for adjuvant HAI. Although prognostic models utilizing clinical and pathologic variables have been associated with survival and overall recurrence, no marker that is prognostic for hepatic recurrence has been established.[4,9–11]

It has been hypothesized that intrahepatic recurrence may arise from occult metastases that are present at the time of resection but are not detectable on conventional imaging.[12,13] Computer-based image analysis, such as texture analysis (TA), has the potential to detect changes in liver parenchymal enhancement. TA quantifies heterogeneity at the pixel level in computed tomography (CT) images. Texture features of liver parenchyma may be altered by occult malignancy and may represent a potential surrogate for later recurrent disease.[14–16] TA of hepatic parenchyma has been shown to be predictive of post-hepatectomy liver insufficiency, hepatitis C activity, and grade of cirrhosis.[17,18] These findings provide preliminary evidence that TA may be able to detect variations in the liver that may, in turn, be related to risk of hepatic recurrence. There may also be a role for TA in the assessment of intratumoral heterogeneity related to cell density, necrosis, and fibrosis. TA has been used to distinguish gastric cancer subtypes[19] and to predict OS in patients with primary colorectal cancers,[20] hepatocellular carcinoma,[21] and CRLM.[22] In patients with CRLM, tumor morphology assessed by radiologists correlated with pathologic response and survival, suggesting a link between imaging, pathology, and survival, but this relationship has not been well-elucidated.[23]

This study analyzed whether TA features of the tumor and future liver remnant (FLR) at the time of hepatic resection are associated with OS and/or HDFS in a large series of consecutive patients undergoing resection for CRLM.

Author Manuscript Author Manuscript Author Manuscript Author Manuscript

METHODS

Population

This retrospective study included 198 patients selected from 384 consecutive patients previously included in an unrelated study.[24] Inclusion criteria were (a) pathologically confirmed resected CRLM, (b) data from pathologic analysis of the nontumoral liver parenchyma, and (c) available preoperative portal venous phase CT images within 6 weeks of hepatic resection. Imaging for 83 patients did not meet quality criteria; these patients were therefore excluded. Patients who died within 90 days of their operation (n=4) or who had <24 months of follow-up (n=11) were also excluded. Additionally, because the pathologic effects of HAI-FUDR on nontumoral liver parenchyma have not been well-described, patients who underwent preoperative HAI-FUDR were excluded (n=33). Finally, to ensure that an accurate 3-D model of the FLR could be obtained, patients who underwent local tumor ablation or >3 wedge resections in the FLR were excluded (n=55). A waiver of Health Insurance Portability and Accountability Act authorization and informed consent was obtained from the Institutional Review Board at our institution.

Data

Demographics, disease characteristics, operative and pathologic data were collected from the database used in the previous study and supplemented via review of patient medical records. Synchronous disease was defined as a diagnosis of CRLM within 6 months of primary colorectal tumor diagnosis. Neoadjuvant chemotherapy was defined as systemic chemotherapy administered within 6 months of liver resection. Adjuvant therapy was offered at the discretion of the multidisciplinary team and consisted of systemic chemotherapy alone or with HAI-FUDR.

Pathology

The pathologic appearance of the nontumoral liver parenchyma had been reassessed by a pathologist in the study mentioned above.[24] Patients were considered to have steatosis if >5% of the examined parenchyma was involved. Steatohepatitis was defined by a nonalcoholic fatty liver disease activity score ≥4 on the basis of the Kleiner-Brunt histologic scoring system.[25] Sinusoidal injury was scored from 0 to 3 on the basis of the Rubbia-Brandt system.[26] Patients with a score ≥1 were considered to have sinusoidal injury.

Tumors were also reassessed by a pathologist in a study examining histologic response patterns in CRLM.[27] Pathologic response was defined as the summation of percentage necrosis, fibrosis, and acellular mucin. Fibrosis >40% had the greatest prognostic significance; the same threshold was used for this study.

CT Acquisition and Image Processing

Patients underwent contrast-enhanced portal venous phase CT scan in accordance with standard imaging protocols. A multidetector CT scanner (Lightspeed 16 and VCT, GE Healthcare, Wisconsin) was used for abdominal imaging, with the following main parameters: autoMA 220–380; noise index 12–14; rotation time 0.7–0.8 milliseconds; scan delay 80 seconds. The post-treatment/preoperative CT was used for patients that received

Author Manuscript Author Manuscript Author Manuscript Author Manuscript

neoadjuvant chemotherapy. In patients with preoperative portal vein embolization (PVE), the pre-PVE CT was used because the effects of PVE on TA are unstudied. Images were transferred from the picture archiving and communication system (PACS) to a workstation for processing. Liver, tumors, vessels, and bile ducts were semi-automatically segmented, and a 3-D model was generated using Scout Liver (Pathfinder Technologies Inc., Tennessee). The performed liver resection was virtually drawn on the 3-D model of the liver. Image volumes of the FLR and index tumor (largest metastasis) were created for TA.

TA

Figure 1 illustrates pixel variation in a hepatic CT scan. Variation in pixel intensity is measured statistically with gray-level co-occurrence matrices (GLCM).[28,29] We generated GLCM statistics using automated software developed by a computer scientist (A.L.S.), as described previously.[17] There are 22 available GLCM features; we chose the five considered, in the literature,[30] to be the most discriminatory: contrast, correlation, energy, entropy, and homogeneity. Definitions of each feature are included in Supplemental Content 1.

Statistical Analysis

Descriptive and comparative statistics were generated using Statistical Software for the Social Sciences (SPSS, version 22.0, IBM, Armonk, New York). A p value of 0.05 was considered significant. Univariable OS and HDFS analysis was performed with Kaplan-Meier statistics (log-rank test) for preoperative clinical and texture variables. Variables with $p<0.1$ were included in a subsequent multivariable model. The OS event was death from any cause, and patients alive at last follow-up were censored. HDFS was defined as the interval from operation to any hepatic recurrence. To test the relationship between clinical and texture variables, Spearman's correlation coefficients were calculated and presented in a correlation matrix. Dependence was ruled out with a correlation coefficient (absolute q value) of <0.7. In the case of dependence between two or more variables, the variable that was the most correlated with OS and HDFS or that was the most clinically relevant was included in multivariable analysis (Cox-regression model) using backward selection. By combining the most significant FLR texture features into a single linear predictor, one FLR texture variable was utilized for the multivariable model. A similar linear predictor was made based on the most significant tumor texture features. Results from the Cox proportional hazards models were reported as hazard ratios (HRs) with 95% confidence intervals (CIs).

RESULTS

Perioperative Data

Overall, 198 patients who underwent hepatic resection for CRLM between April 2003 and March 2007 were included in the study. The median age of patients was 61 years (range, 30–88 years), and 60% (n=118) were male. Demographic and clinicopathologic factors are listed in Table 1. A Spearman's correlation matrix demonstrating the statistical relationship between clinicopathologic factors and texture variables is presented in Supplemental Content 2.

Author Manuscript Author Manuscript Author Manuscript Author Manuscript

OS

Median OS for the entire cohort was 75.7 months (95% CI, 60.7–90.7 months). After a median follow-up of 102 months (range, 3.8–131.9 months), 90 patients (45.5%) were alive and 70 had no evidence of disease. In univariable analysis, tumor size, extrahepatic disease, neoadjuvant chemotherapy, tumor fibrosis >40%, FLR homogeneity, FLR contrast, FLR energy, FLR entropy, tumor correlation, tumor homogeneity, and tumor contrast ($p<0.1$; Table 2) were associated with OS and subsequently included in a multivariable Cox-regression model. Following Spearman's test for dependence (Supplemental Content 2), FLR homogeneity and FLR contrast were highly correlated with FLR energy and therefore removed from the model. FLR energy and FLR entropy were combined into a single linear predictor, "FLR texture signal," which was included in the multivariable model. Tumor correlation and tumor contrast were similarly combined, as "tumor texture signal," and included in the multivariable model. Neoadjuvant chemotherapy, extrahepatic disease, tumor fibrosis >40%, FLR texture signal, and tumor texture signal were independently associated with OS (Table 3).

HDFS

At the last follow-up, overall recurrence was 66.7% ($n=132$); 81 patients with recurrence (61.4%) had liver involvement, and recurrence was confined to the liver in 43 patients. Median overall recurrence-free survival was 22 months (95% CI, 14.0–30.6 months); median HDFS was not reached. In univariable analysis, multiple metastases, preoperative PVE, extrahepatic disease, tumor fibrosis >40%, FLR energy, FLR entropy, tumor correlation, and tumor contrast ($p<0.1$; Table 2) were associated with HDFS (as above, FLR homogeneity and FLR contrast were excluded). These factors and FLR and tumor texture signals were subsequently included in a multivariable Cox-regression model. Extrahepatic disease and FLR texture signal were independently associated with HDFS (Table 3). By dichotomizing FLR texture signal into high and low texture (using the median value), we were able to stratify patients into two distinct risk groups of liver recurrence (Figure 2A). Patients with a high FLR texture signal had a significantly higher cumulative risk of liver recurrence (HR, 2.09; 95% CI, 1.33–3.28; $p=0.001$). The cumulative hazard of liver recurrence at 24 months after resection for CRLM was 41.1% (95% CI, 30.5% 50.2%) in the high-risk FLR group and 19.5% (95% CI, 11.1% 27.0%) in the low-risk FLR group. There was no difference between the high-risk and low-risk groups with regard to clinical risk score ($p=0.112$).

Impact of Adjuvant HAI-FUDR Therapy

The administration of adjuvant HAI-FUDR was associated with improved HDFS (HR, 0.591; 95% CI, 0.36–0.98; $p=0.034$; Figure 2B). FLR texture signal, dichotomized and grouped by HAI-FUDR, was used to stratify patients into distinct risk groups of recurrence (Figure 2C). The administration of pump therapy did not alter the strength of the association between FLR texture signal and HDFS in a subset analysis (HAI-FUDR: HR, 1.81; 95% CI, 0.73–4.42; no HAI-FUDR: HR, 2.20; 95% CI, 1.30–3.69; $p=0.196$).

Author Manuscript Author Manuscript Author Manuscript Author Manuscript

DISCUSSION

This study investigated the use of TA to predict survival and hepatic recurrence in a consecutive series of patients undergoing hepatic resection for CRLM. In a multivariable analysis that included standard preoperative clinical variables, tumor and FLR texture signals were associated with OS. FLR texture signal was associated with HDFS. These findings suggest that preoperative TA of the tumor and nontumoral liver represent potential imaging biomarkers for patients undergoing hepatic resection for CRLM.

With regard to TA of the liver parenchyma, higher FLR texture signal was associated with shorter survival. In other words, high FLR texture signal corresponded to a homogeneous FLR appearance with limited pixel variation on CT. Using FLR texture signal as a dichotomized variable allowed stratification of patients into two distinct groups (Figure 2A). Patients with high-risk FLR had shorter HDFS. Thus, high FLR texture signal might suggest the presence of occult metastases or other underlying parenchymal changes that are associated with recurrence. Structural changes (angiogenesis, extracellular matrix remodeling) in the remote and peritumoral liver parenchyma have been described in patients with CRLM.[31–33] It has also been shown that exosomes derived from pancreatic ductal adenocarcinoma induce changes in the extracellular matrix, providing a favorable niche for development of metastasis in the liver.[34] These parenchymal modifications involved in prometastatic mechanisms might already be occurring in the FLR at the time of resection and may be detectable using preoperative TA. However, the factors underlying the association between homogeneous FLR and shorter survival require further investigation.

Texture features of the FLR were correlated with some clinical variables. Notably, steatosis and steatohepatitis were correlated with FLR texture features. However, underlying steatosis and steatohepatitis were not associated with OS and HDFS in univariable analysis. Thus, although steatosis and steatohepatitis may contribute to alterations in the appearance of the FLR, they do not account for differences in OS and HDFS. Validation of such assumptions will require further investigations that pair preoperative TA with pathologic assessment of the FLR.

Analysis of our institutional data shows there is a benefit associated with adjuvant HAI-FUDR after resection for CRLM.[7] In this study, approximately 40% of patients who received adjuvant chemotherapy also received HAI-FUDR. In this cohort, adjuvant HAI-FUDR modified the risk of liver recurrence, and this finding was consistent with those of previous clinical trials.[7,35] HAI-FUDR was associated with improved HDFS, regardless of high or low texture signal. HAI-FUDR may be an effective treatment strategy for patients with a high risk of hepatic recurrence.

Homogenous tumors were associated with worse outcomes, which is consistent with trends observed in a study by Lubner et al.[22] Based on radiographic assessment, Chun et al. showed that transition from a uniformly heterogenous tumor appearance to a homogeneous tumor appearance was associated with improved survival and pathologic response following neoadjuvant chemotherapy.[23] In our study, tumor fibrosis >40% and tumor texture signal were associated with OS ($p<0.05$) and trends in HDFS ($p<0.10$).

Author Manuscript Author Manuscript Author Manuscript Author Manuscript

Extrahepatic disease was also independently associated with OS and HDFS, concordant with previous results.[4,10,36–38] Largest metastasis size was associated with OS in univariable analysis, as in previous series, but this finding did not hold in multivariable analysis.[4,9,10,36,37] In univariable analysis, neoadjuvant therapy was associated with worse OS. This variable was included in multivariable analysis, but the suitability for inclusion is debatable. First, neoadjuvant therapy was delivered selectively, mostly on the basis of worrisome clinical features (size, multifocality, or extrahepatic disease), and likely reflected the burden of metastatic disease. Second, tumor response to neoadjuvant chemotherapy is associated with prognosis, whereas neoadjuvant chemotherapy alone does not result in tumor response.[39] In our data set, pathologic response was scored for all tumors regardless of chemotherapy status. Fibrosis >40% has been shown to drive the improvement in disease-specific survival in patients treated with neoadjuvant chemotherapy.[27] This variable remained true for OS, although total response >75% did not reach significance.

This study has several limitations. First, selection bias is inherent in the retrospective nature of the study. Therefore, both external validation and, optimally, a prospective trial are needed to validate these results. TA remains a nonvalidated marker in the investigational stage but, if validated, has the potential to impact patient selection for specific therapies. Nevertheless, our cohort was the largest ever explored for liver TA, and the follow-up was extensive. The same CT acquisition protocol has been in place at our institution since 2002, so the rationale for including patients from 2003 to 2007 was to allow sufficient time to assess long-term recurrence and survival. Second, although a pathologist reviewed the resected nontumoral liver parenchyma, the grading of steatosis and steatohepatitis is potentially subject to sampling error, limiting correlation with texture features averaged over the entire FLR. In the same way, tumor fibrosis, necrosis, and mucin were also vulnerable to sampling error. Further studies to explain the correlation between texture values and pathology are needed. Finally, TA of CRLM is currently limited to high-volume medical centers with the infrastructure to support quantitative image analysis. However, we intentionally used routine preoperative CT images, a modality available at most institutions, so that the analysis could be automated in the future and made more widely applicable to general practice.

In conclusion, tumoral and parenchymal differences on routine portal venous phase CT imaging can be quantified by analysis of underlying pixel variation. Imaging features were independently associated with survival and hepatic recurrence suggesting that TA of the liver is worthy of further validation as a potential biomarker.

Supplementary Material

Refer to Web version on PubMed Central for supplementary material.

Acknowledgments

Funding: This study was supported in part by NIH/NCI Cancer Center Support Grant P30 CA008748. Alexandre Doussot received research fellowship grants from the French Association of Hepatobiliary Surgery and Transplantation and from Université de Bourgogne.

Author Manuscript Author Manuscript Author Manuscript Author Manuscript

References

1. Siegel R, DeSantis C, Virgo K, et al. Cancer treatment and survivorship statistics, 2012. CA Cancer J Clin. 2012; 62(4):220–41. [PubMed: 22700443]
2. Mella J, Biffin A, Radcliffe AG, et al. Population-based audit of colorectal cancer management in two UK health regions. Colorectal Cancer Working Group, Royal College of Surgeons of England Clinical Epidemiology and Audit Unit. Br J Surg. 1997; 84(12):1731–6. [PubMed: 9448628]
3. Tomlinson JS, Jarnagin WR, DeMatteo RP, et al. Actual 10-year survival after resection of colorectal liver metastases defines cure. J Clin Oncol. 2007; 25(29):4575–80. [PubMed: 17925551]
4. Fong Y, Fortner J, Sun RL, et al. Clinical score for predicting recurrence after hepatic resection for metastatic colorectal cancer: analysis of 1001 consecutive cases. Ann Surg. 1999; 230(3):309–18. discussion 318–21. [PubMed: 10493478]
5. House MG, Ito H, Gonen M, et al. Survival after hepatic resection for metastatic colorectal cancer: trends in outcomes for 1,600 patients during two decades at a single institution. J Am Coll Surg. 2010; 210(5):744–52. 752–5. [PubMed: 20421043]
6. D'Angelica M, Kornprat P, Gonen M, et al. Effect on outcome of recurrence patterns after hepatectomy for colorectal metastases. Ann Surg Oncol. 2011; 18(4):1096–103. [PubMed: 21042942]
7. Kemeny N, Huang Y, Cohen AM, et al. Hepatic arterial infusion of chemotherapy after resection of hepatic metastases from colorectal cancer. N Engl J Med. 1999; 341(27):2039–48. [PubMed: 10615075]
8. Goere D, Benhaim L, Bonnet S, et al. Adjuvant chemotherapy after resection of colorectal liver metastases in patients at high risk of hepatic recurrence: a comparative study between hepatic arterial infusion of oxaliplatin and modern systemic chemotherapy. Ann Surg. 2013; 257(1):114–20. [PubMed: 23235397]
9. Nordlinger B, Guiguet M, Vaillant JC, et al. Surgical resection of colorectal carcinoma metastases to the liver. A prognostic scoring system to improve case selection, based on 1568 patients. Association Francaise de Chirurgie. Cancer. 1996; 77(7):1254–62. [PubMed: 8608500]
10. Rees M, Tekkis PP, Welsh FK, et al. Evaluation of long-term survival after hepatic resection for metastatic colorectal cancer: a multifactorial model of 929 patients. Ann Surg. 2008; 247(1):125–35. [PubMed: 18156932]
11. Zakaria S, Donohue JH, Que FG, et al. Hepatic resection for colorectal metastases: value for risk scoring systems? Ann Surg. 2007; 246(2):183–91. [PubMed: 17667495]
12. Leen E. The detection of occult liver metastases of colorectal carcinoma. J Hepatobiliary Pancreat Surg. 1999; 6(1):7–15. [PubMed: 10436232]
13. Conzelmann M, Linnemann U, Berger MR. Detection of disseminated tumour cells in the liver of colorectal cancer patients. Eur J Surg Oncol. 2005; 31(1):38–44. [PubMed: 15642424]
14. Rao SX, Lambregts DM, Schnerr RS, et al. Whole-liver CT texture analysis in colorectal cancer: Does the presence of liver metastases affect the texture of the remaining liver? United European Gastroenterol J. 2014; 2(6):530–8.
15. Ganeshan B, Miles KA, Young RC, et al. Hepatic entropy and uniformity: additional parameters that can potentially increase the effectiveness of contrast enhancement during abdominal CT. Clin Radiol. 2007; 62(8):761–8. [PubMed: 17604764]
16. Miles KA, Ganeshan B, Griffiths MR, et al. Colorectal cancer: texture analysis of portal phase hepatic CT images as a potential marker of survival. Radiology. 2009; 250(2):444–52. [PubMed: 19164695]
17. Simpson AL, Adams LB, Allen PJ, et al. Texture analysis of preoperative CT images for prediction of postoperative hepatic insufficiency: a preliminary study. J Am Coll Surg. 2015; 220(3):339–46. [PubMed: 25537305]
18. Wu Z, Matsui O, Kitao A, et al. Hepatitis C related chronic liver cirrhosis: feasibility of texture analysis of MR images for classification of fibrosis stage and necroinflammatory activity grade. PLoS One. 2015; 10(3):e0118297. [PubMed: 25742285]
19. Ba-Ssalamah A, Muin D, Schernthaner R, et al. Texture-based classification of different gastric tumors at contrast-enhanced CT. Eur J Radiol. 2013; 82(10):e537–43. [PubMed: 23910996]

Author Manuscript Author Manuscript Author Manuscript Author Manuscript

20. Ng F, Ganeshan B, Kozarski R, et al. Assessment of primary colorectal cancer heterogeneity by using whole-tumor texture analysis: contrast-enhanced CT texture as a biomarker of 5-year survival. Radiology. 2013; 266(1):177–84. [PubMed: 23151829]
21. Hayano K, Yoshida H, Zhu AX, et al. Fractal analysis of contrast-enhanced CT images to predict survival of patients with hepatocellular carcinoma treated with sunitinib. Dig Dis Sci. 2014; 59(8): 1996–2003. [PubMed: 24563237]
22. Lubner MG, Stabo N, Lubner SJ, et al. CT textural analysis of hepatic metastatic colorectal cancer: pre-treatment tumor heterogeneity correlates with pathology and clinical outcomes. Abdom Imaging. 2015; 40(7):2331–7. [PubMed: 25968046]
23. Chun YS, Vauthey JN, Boonsirikamchai P, et al. Association of computed tomography morphologic criteria with pathologic response and survival in patients treated with bevacizumab for colorectal liver metastases. JAMA. 2009; 302(21):2338–44. [PubMed: 19952320]
24. Wolf PS, Park JO, Bao F, et al. Preoperative chemotherapy and the risk of hepatotoxicity and morbidity after liver resection for metastatic colorectal cancer: a single institution experience. J Am Coll Surg. 2013; 216(1):41–9. [PubMed: 23041049]
25. Kleiner DE, Brunt EM, Van Natta M, et al. Design and validation of a histological scoring system for nonalcoholic fatty liver disease. Hepatology. 2005; 41(6):1313–21. [PubMed: 15915461]
26. Rubbia-Brandt L, Audard V, Sartoretti P, et al. Severe hepatic sinusoidal obstruction associated with oxaliplatin-based chemotherapy in patients with metastatic colorectal cancer. Ann Oncol. 2004; 15(3):460–6. [PubMed: 14998849]
27. Poultsides GA, Bao F, Servais EL, et al. Pathologic response to preoperative chemotherapy in colorectal liver metastases: fibrosis, not necrosis, predicts outcome. Ann Surg Oncol. 2012; 19(9): 2797–804. [PubMed: 22476753]
28. Haralick RM, Shanmuga K, Dinstein I. Textural Features for Image Classification. Ieee Transactions on Systems Man and Cybernetics. 1973; Smc3(6):610–621.
29. Haralick RM. Statistical and Structural Approaches to Texture. Proceedings of the Ieee. 1979; 67(5):786–804.
30. Soh LK, Tsatsoulis C. Texture analysis of SAR sea ice imagery using gray level co-occurrence matrices. Ieee Transactions on Geoscience and Remote Sensing. 1999; 37(2):780–795.
31. van der Wal GE, Gouw AS, Kamps JA, et al. Angiogenesis in synchronous and metachronous colorectal liver metastases: the liver as a permissive soil. Ann Surg. 2012; 255(1):86–94. [PubMed: 22156924]
32. van der Wal GE, Gouw AS, Kamps JA, et al. Reply to letter: "Markers of angiogenesis in synchronous and in metachronous colorectal hepatic metastases". Ann Surg. 2015; 261(1):e20–1.
33. Eveno C, Hainaud P, Rampanou A, et al. Proof of prometastatic niche induction by hepatic stellate cells. J Surg Res. 2015; 194(2):496–504. [PubMed: 25528682]
34. Costa-Silva B, Aiello NM, Ocean AJ, et al. Pancreatic cancer exosomes initiate pre-metastatic niche formation in the liver. Nat Cell Biol. 2015; 17(6):816–26. [PubMed: 25985394]
35. Lorenz M, Muller HH, Schramm H, et al. Randomized trial of surgery versus surgery followed by adjuvant hepatic arterial infusion with 5-fluorouracil and folinic acid for liver metastases of colorectal cancer. German Cooperative on Liver Metastases (Arbeitsgruppe Lebermetastasen). Ann Surg. 1998; 228(6):756–62. [PubMed: 9860474]
36. Yamaguchi T, Mori T, Takahashi K, et al. A new classification system for liver metastases from colorectal cancer in Japanese multicenter analysis. Hepatogastroenterology. 2008; 55(81):173–8. [PubMed: 18507101]
37. Iwatsuki S, Dvorchik I, Madariaga JR, et al. Hepatic resection for metastatic colorectal adenocarcinoma: a proposal of a prognostic scoring system. J Am Coll Surg. 1999; 189(3):291–9. [PubMed: 10472930]
38. Kanemitsu Y, Kato T. Prognostic models for predicting death after hepatectomy in individuals with hepatic metastases from colorectal cancer. World J Surg. 2008; 32(6):1097–107. [PubMed: 18200429]
39. Allen PJ, Kemeny N, Jarnagin W, et al. Importance of response to neoadjuvant chemotherapy in patients undergoing resection of synchronous colorectal liver metastases. J Gastrointest Surg. 2003; 7(1):109–15. discussion 116–7. [PubMed: 12559192]

Author Manuscript Author Manuscript Author Manuscript Author Manuscript

Synopsis

In patients with CRLM, tumor and parenchymal differences on CT imaging can be quantified by texture analysis (TA) of underlying pixel variation. Imaging features were associated with survival and hepatic recurrence suggesting that TA is worthy of further validation as a potential biomarker.

Author Manuscript Author Manuscript Author Manuscript Author Manuscript

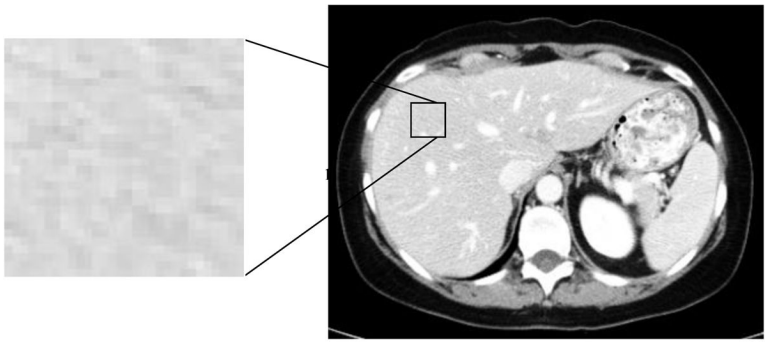

Figure 1.

Underlying variation in pixel intensity in an exemplar 30 x 30 pixel patch derived from a liver CT scan. Texture analysis quantifies this variation. In this study, texture was extracted from the entire FLR and index tumor.

Author Manuscript Author Manuscript Author Manuscript Author Manuscript

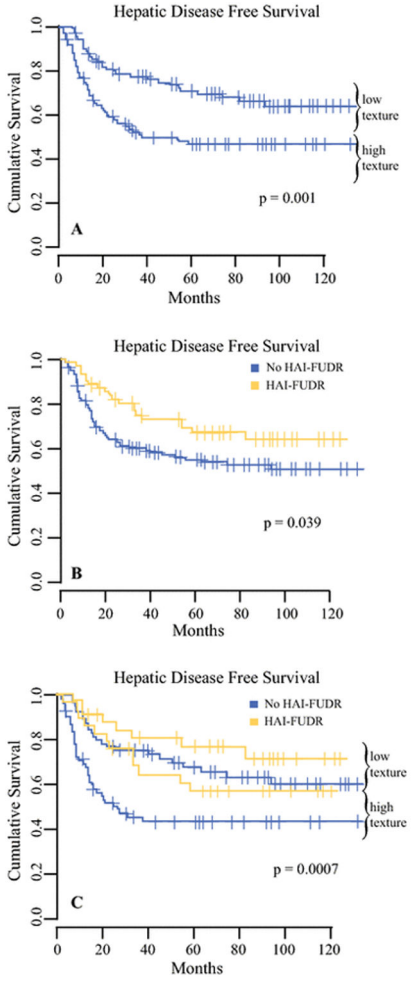

Figure 2.

Kaplan-Meier curve of hepatic disease-free survival in patients stratified by (A) FLR texture, (B) adjuvant therapy, and (C) adjuvant therapy and FLR texture. Sixty-two patients received HAI-FUDR and systemic chemotherapy, and 136 patients received no adjuvant HAI-FUDR.

Author Manuscript Author Manuscript Author Manuscript Author Manuscript

Table 1

Demographic, clinicopathologic, and texture features of the study population (N=198)

	Value
Male sex, *n* (%)	118 (60)
Age, years (range)	61 (30–88)
Major comorbidity, *n* (%)	110 (56)
Body mass index, kg/m^2 (range)	26.8 (17.2–44.3)
Node-positive primary tumor, *n* (%)	69 (35)
Synchronous CRLM, *n* (%)	112 (57)
Multiple metastases, *n* (%)	114 (58)
CRS (score 0–2), n (%)	118 (60)
CEA >200, *n* (%)	3 (1.5)
Maximal tumor size, cm, mean ± SD	3.5 ± 2.6
Bilobar disease, *n* (%)	86 (43)
Extrahepatic disease, *n* (%)	17 (9)
Neoadjuvant chemotherapy, *n* (%)	122 (62)
Preoperative PVE, *n* (%)	23 (12)
Pathology of nontumoral liver, *n* (%)	
Steatosis	68 (34)
Sinusoidal dilation	26 (13)
Steatohepatitis (grade ≥4)	7 (4)
Pathology of index tumor	
Total response >75%, *n* (%)	38 (19)
Tumor fibrosis >40%, *n* (%)	24 (12)
Percentage necrosis, median (range)	30 (0–90)
Percentage fibrosis, median (range)	10 (0–100)
Percentage mucin, median (range)	0 (0–100)
Texture features, mean ± SD	
FLR correlation	0.028 ± 0.025
FLR homogeneity	0.719 ± 0.064
FLR contrast	0.895 ± 0.375
FLR energy	0.239 ± 0.133
FLR entropy	0.469 ± 0.157
Tumor correlation	0.274 ± 0.156
Tumor homogeneity	0.629 ± 0.077
Tumor contrast	1.780 ± 0.843
Tumor energy	0.111 ± 0.088
Tumor entropy	0.052 ± 0.065

CRLM colorectal liver metastases, *CRS* clinical risk score, *CEA* carcinoembryonic antigen, *PVE* portal vein embolization, *FLR* future liver remnant

Author Manuscript Author Manuscript Author Manuscript Author Manuscript

Ann Surg Oncol. Author manuscript; available in PMC 2018 September 01.

Table 2

Predictors of overall survival and recurrence in univariable analysis (N=198)

	OS, months, median (95% CI)	HR (95% CI)	*p* value	3-year HDFS, *n* (%)	HR (95% CI)	*p* value
Male sex	82.0 (63.0–101.0)	—	0.184	68 (34)	—	0.341
Age	—	1.00 (0.99–1.02)	0.963	—	0.99 (0.97–1.01)	0.190
Major comorbidity	80.7 (54.9–106.5)	—	0.531	62 (31)	—	0.759
Body mass index	—	0.97 (0.94–1.01)	0.177	—	0.97 (0.92–1.01)	0.130
Node-positive primary tumor	80.7 (55.2–106.2)	—	0.947	37 (19)	—	0.777
Synchronous CRLM	80.7 (51.7–109.8)	—	0.349	59 (30)	—	0.648
Multiple metastases	67.6 (57.4–77.8)	—	0.118	57 (29)	—	**0.066**
CEA >200	26.8 ( )	—	0.288	—	—	0.783
Maximal tumor size	—	1.08 (1.02–1.15)	**0.014**	—	1.02 (0.94–1.11)	0.590
Bilobar disease	72.5 (61.7–83.4)	—	0.588	45 (23)	—	0.749
Extrahepatic disease	36.2 (28.6–43.8)	—	**0.003**	4 (2)	—	**0.004**
Neoadjuvant chemotherapy	65.3 (56.3–74.4)	—	**0.003**	58 (29)	—	0.146
Preoperative PVE	75.7 (40.8–110.5)	—	0.799	8 (4)	—	**0.016**
Steatosis	98.9 (62.3–135.5)	—	0.121	40 (20)	—	0.561
Sinusoidal dilation	75.3 (54.3–96.3)	—	0.783	14 (7)	—	0.464
Steatohepatitis (grade ≥4)	68.1 (30.5–105.6)	—	0.680	4 (2)	—	0.871
Tumor total response >75%	108.5 (79.4–137.6)	—	0.119	22 (11)	—	0.584
Tumor fibrosis >40%	—	—	**0.031**	15 (8)	—	**0.059**
Percentage tumor necrosis	—	0.99 (0.99–1.01)	0.865	—	1.00 (0.99–1.01)	0.899
Percentage fibrosis	—	0.99 (0.98–1.00)	0.146	—	0.99 (0.98–1.00)	0.192
Percentage tumor mucin	—	0.98 (0.99–1.01)	0.592	—	1.00 (0.98–1.01)	0.672
FLR correlation	—	4.76 (0.01–4347)	0.654	—	3.12 (0.00–18546)	0.797
FLR homogeneity	—	18.73 (1.29–271.1)	**0.032**	—	70.24 (3.56–1384)	**0.005**
FLR contrast	—	0.56 (0.31–1.01)	**0.055**	—	0.50 (0.25–1.00)	**0.050**
FLR energy	—	3.20 (0.93–11.01)	**0.065**	—	6.36 (1.74–23.29)	**0.005**
FLR entropy	—	0.20 (0.06–0.72)	**0.014**	—	0.16 (0.04–0.72)	**0.017**
Tumor correlation	—	5.24 (1.58–17.42)	**0.007**	—	6.02 (1.51–24.03)	**0.011**
Tumor homogeneity	—	8.47 (1.14–63.10)	**0.037**	—	5.23 (0.46–59.44)	0.183

Author Manuscript Author Manuscript Author Manuscript Author Manuscript

	OS, months, median (95% CI)	HR (95% CI)	*p* value	3-year HDFS, *n* (%)	HR (95% CI)	*p* value
Tumor contrast	—	0.73 (0.58–0.92)	**0.009**	—	0.78 (0.60–1.03)	**0.078**
Tumor energy	—	1.81 (0.37–8.84)	0.463	—	1.31 (0.17–10.24)	0.796
Tumor entropy	—	5.61 (0.51–61.54)	0.158	—	0.54 (0.02–16.03)	0.722

OS overall survival, *HDFS* hepatic disease-free survival, *CRLM* colorectal liver metastases, *CEA* carcinoembryonic antigen, *PVE* portal vein embolization, *FLR* future liver remnant

Author Manuscript

Author Manuscript

Author Manuscript

Author Manuscript

Table 3

Results of multivariable Cox analysis of predictors of survival and recurrence

	OS, HR (95% CI)	*p* value	HDFS, HR (95% CI)	*p* value
Full model				
Maximal tumor size	1.02 (0.95–1.10)	0.515	—	—
Multiple metastases	—	—	1.44 (0.90–2.32)	0.131
Extrahepatic disease	2.19 (1.15–4.16)	**0.036**	2.25 (1.16–4.34)	**0.016**
Preoperative PVE	—		1.62 (0.86–3.04)	0.136
Neoadjuvant chemotherapy	1.83 (1.20–2.78)	**0.005**	—	—
Tumor fibrosis >40%	0.45 (0.21–0.98)	**0.045**	0.42 (0.17–1.05)	**0.063**
FLR texture signal	2.19 (1.09–4.40)	**0.028**	1.94 (1.02–3.69)	**0.044**
Tumor texture signal	2.08 (0.97–4.45)	**0.081**	2.2 (1.02–5.02)	**0.045**
Final model				
Extrahepatic disease	2.25 (1.21–4.17)	**0.010**	2.39 (1.25–4.57)	**0.008**
Neoadjuvant chemotherapy	1.84 (1.21–2.80)	**0.005**	—	—
Tumor fibrosis >40%	0.46 (0.21–1.00)	**0.049**	0.45 (0.18–1.12)	**0.086**
FLR texture signal	2.15 (1.08– 4.29)	**0.029**	2.21 (1.21–4.03)	**0.010**
Tumor texture signal	2.35 (1.21–4.55)	**0.013**	2.09 (0.95–4.58)	**0.066**

OS overall survival, *HDFS* hepatic disease-free survival, *PVE* portal vein embolization, *FLR* future liver remnant